TOWARDS AN EFFICIENT, ROBUST AND ACCURATE SOLVER FOR SUPERSONIC VISCOUS FLOWS

T J Birch*, D K Ludlow and N Qin****

***DERA, Bedford, Bedfordshire, UK**
****Cranfield University, Bedfordshire, UK**

Keywords: *CFD, PNS, Missile aerodynamic.*

Abstract

Recent progress made towards the development of an efficient multizone parabolized Navier-Stokes solver for missile and projectile configurations is described. Results for three test cases are presented and compared with wind tunnel data to illustrate the predictive capabilities of the solver. The solver provides a rapid means of obtaining viscous flow solutions on configurations of practical interest, and the results obtained compare well with measured data.

1 Introduction

Computational fluid dynamics (CFD) is having an increasing impact on the aerodynamic assessment of air vehicles. The use of inviscid CFD methods for the prediction of airframe forces and moments is now very common, and a large number of different solution strategies and codes are available. However, although capable of providing good predictions for a wide range of configurations at low and moderate angles of incidence, inviscid methods can be unreliable at high incidence when viscous effects become important.

The Reynolds-averaged Navier-Stokes (RANS) equations can describe all of the flow physics of interest to the aerodynamicist and are applicable over the range of Mach numbers from subsonic to hypersonic. However, obtaining numerical solutions can be expensive in terms of both computer memory and execution times, and currently it is not feasible to use the RANS approach to populate aerodynamic databases due to the high cost per polar.

The numerical solution of the Parabolized Navier-Stokes (PNS) equations provides an efficient means of obtaining viscous flow solutions for air vehicles operating at supersonic and hypersonic Mach numbers, and represents an attractive alternative to a time-marching Reynolds-averaged Navier-Stokes approach. The PNS equations retain the ability to model important viscous effects and enable the use of a space-marching strategy which considerably reduces both computer execution times and memory requirements.

This paper describes the recent progress made towards the development of an efficient PNS solver for missile and projectile configurations of practical interest. The project is a 3-year programme involving DERA, Cranfield University, Matra BAe Dynamics and SAAB Dynamics.

2 Solver Description

The implicit multizone PNS solver described in this section has evolved over a number of years [1-4] and has been developed primarily for predicting the aerodynamic characteristics of missiles and projectiles travelling at supersonic speeds. The governing flow equations are the steady-state compressible Navier-Stokes equations. The perfect gas law and Sutherland's law for laminar viscosity close the system. When necessary, turbulence is simulated by the Favre mass-averaged form of the Navier-Stokes equations with a Baldwin-Lomax [5] algebraic turbulence model, enhanced to account for

© Crown copyright 2000. Published by the International Council of the Aeronautical Sciences with the permission of the Defence Evaluation and Research Agency on behalf of the Controller of HMSO.

crossflow separation by modifications due to either Degani-Schiff [6] or the curvature method of Qin and Jayatunga [7]. For cases where viscous effects are unimportant, the viscosity may be switched off and the corresponding Euler equations may be solved with appropriate boundary conditions.

The governing flow equations are discretised using a cell-centred finite-volume scheme in a generalised coordinate system for use with structured, body-conforming grids. In order to enable a stable well-defined space-marching solution routine, the discretised flow equations are parabolized by use of the following assumptions: (i) Viscous terms in the streamwise direction are negligible compared to their counterparts in the cross-flow direction. (ii) The flow outside the boundary layer is supersonic in the streamwise direction and a portion of the streamwise (momentum) pressure gradient within subsonic regions is negligible.

Several interpretations of the parabolising approximation by Vigneron *et al*., [8] in which a portion, $(1-\omega)$, of the streamwise pressure gradient is neglected, have been investigated and implemented within the current solver (ω is a function of the local streamwise Mach number). The two main forms are: (i) The flux-conservative scheme where $\Delta_\xi[(1-\omega)p\mathrm{d}\boldsymbol{s}]$ has been subtracted from the momentum based flow-governing equations. (ii) The grid-conservative scheme proposed by Morrison and Korte [9], where $(1-\omega)\mathrm{d}\boldsymbol{s}\Delta_\xi p$ has been subtracted from the momentum based flow-governing equations. The interpretation proposed by Morrison and Korte was found to reproduce more exactly the boundary layer profile on a flat-plate, at a cost of up-to double the computational time. However in problems with non-zero pressure gradient, there seemed little difference between the results obtained by the two methods. Often a more accurate boundary-layer profile was obtained by adding back the subtracted term, but evaluated at the previous streamwise station. However, unlike the two schemes above, this produces a scheme that is undesirably unstable with small streamwise cell size.

A first-order streamwise flux is determined from the values of the flow-variables at the cell-centre immediately upstream of the interface. Streamwise accuracy can be improved to second order outside of the boundary layer by use of a (non slope-limited) primitive variable extrapolation. The FLARE approximation [10] is included for stabilising the marching routine in small regions of streamwise flow reversal.

In the crossflow plane, the inviscid flux function is discretised by the approximate Riemann solver of Osher and Solomon [11] with physical ordering. Spatial accuracy is enhanced to nominally third order by a MUSCL primitive variable extrapolation scheme, cf. [12]. The differentiable slope-limiter of Anderson *et al*. [12] is included to avoid spurious oscillations in regions of sharp gradients. The viscous flux function is determined using a second order central scheme. Consequently, the derivative of the resulting scheme with respect to the flow variables is continuous for laminar flows.

The current space-marching scheme comprises of a single-sweep from the upstream to the downstream boundary, where on each cross-flow plane the PNS equations form an implicit equation for the flow variables at that station. To solve for these flow variables, a pseudo-time term is added to the equations and they are iteratively solved by pseudo time relaxation. Unlike non-iterative space-marching schemes, there is no stability restriction on the maximum size of the spatial step-size. In order to accelerate the pseudo time relaxation, one or a combination of Multigrid and Implicit pseudo time marching strategies can be used.

Currently the implicit pseudo time iteration is based upon one of two schemes: Directional Approximate Factorisation (DAF), or Block Incomplete Lower-Upper Factorisation (BILUF). These factorisations can either be used on their own or as preconditioning matrices for a restarted GMRES scheme [13]. In the GMRES scheme, the Jacobian-vector products may be evaluated directly or by matrix-free finite differences [14]. The matrix-free scheme saves the storage of one Jacobian size matrix at the expense of about a 10 percent

increase in computational time. Where they are required, the components of the Jacobian matrix are evaluated analytically from the continuous derivatives of the flux functions. Derivatives of the turbulent viscosity are ignored everywhere, because of its non-differentiability.

The Full Approximation Multigrid Scheme as proposed by Brandt [15], using weighted summation restriction operators and bilinear interpolation prolongation is utilised. Multigrid can be performed on up-to three levels of grid refinement.

In order to enable the prediction of realistic geometries, a multiblock technique is used. This allows non-matching grids between streamwise blocks by using a non-flux conservative bilinear interpolation. Within a cross-flow plane the block boundaries must be matching. In the implicit schemes, Jacobian contributions across grid interface boundaries are ignored and the matrices are stored and inverted one grid block at a time. The flow-field is updated only when the linear system has been solved on all grid blocks in the plane.

3 Results

In this section, results are presented for three test cases of increasing geometric complexity. In each case comprehensive experimental data, consisting of surface pressure, flowfield and forces, are available.

The first test case consists of an axisymmetric body having a 3 calibre tangent-ogive nose followed by a cylindrical section. The flow conditions for this case were:

$$M=2,\ \sigma=10^{o},\ Re_D=1.2 \times 10^6$$

Although geometrically simple the flow physics associated with this case are complex and represent a significant challenge. Experimental data for this case and a suitable computational grid were provided by ONERA[16]. The grid consisted of 60 streamwise planes with 85 radial and 73 circumferential grid points in each plane. The execution time for this test case was less than 30 minutes on a 180 MHz R10000 processor when using the BILUF iterative scheme.

The measured flowfield at x/D=9 is compared with predictions, obtained using both the Degani-Schiff and curvature turbulence modelling options, in Figure 1. The primary body vortex is in good qualitative agreement with experiment in both cases. However, the results obtained using the curvature model represent a small improvement over the Degani-Schiff results. This improvement is also evident in Figure 2, which compares measured and predicted circumferential pressure distributions. Figure 3 shows the measured and predicted forces and moments as a function of x/D. The results obtained with the curvature model are in excellent agreement with experiment, whereas the Degani-Schiff results underpredict both normal force coefficient and the axial centre of pressure beyond x/D=6.

The second test case consists of an axisymmetric body plus a cruciform delta wing. This model has been studied extensively in the wind tunnels at DERA Bedford over a range of flow conditions. The flow conditions for this case were:

$$M=2.5,\ \sigma=14^{o},\ Re_D= 1.23 \times 10^6$$

A multiblock grid consisting of 226 streamwise planes and approximately 2.5 x 10^6 grid points was used for the computation. The execution time was less than 4.5 hours on a 180 MHz R10000 processor when using the DAF preconditioned GMRES scheme.

Figure 4 shows a comparison between measured and predicted surface pressures. The two sets of results are in good agreement. The overall forces and moments are compared in Table 1. The predicted normal force coefficient and longitudinal centre of pressure are within 2% of experiment. The axial force coefficient, however, has been seriously underpredicted. Although, the value of Cx obtained using the PNS code does represent a significant improvement when compared with the result obtained in Euler mode, where Cx=0.15.

	C_Z	Xcp	C_X
EXP	4.41	7.37	0.34
PNS	4.49	7.41	0.26
Error	+1.8%	+0.5%	-23%

Table 1. Measured and predicted loads on body-wing at M=2.5, σ=14°.

The flowfield in a crossflow plane positioned at x/D=11.5 is plotted in Figure 5 in the form of pitot pressure ratio. Despite the complexity of the flowfield at this position, which is just downstream of the wing trailing edge, all of the important flow features have been predicted. These include shock waves, multiple body and wing vortices. The accurate prediction of such features is vital particularly if downstream aerodynamic surfaces are employed, as these would be immersed in this complex flowfield.

The final test case consists of the body-wing configuration previously discussed, with a set of cruciform control surfaces positioned near the nose. PNS results have been obtained for this configuration at M=2.5, Re_D= 1.23 x 10^6 over the incidence range σ=0° to 14° both with and without control deflections. A grid consisting of 6 non-matching streamwise blocks was generated using the SAAB Dynamics code Gemini [17]. The total number of cells was approximately 2 x10^6.

The computed surface pressure distribution and density contours on the symmetry plane are presented in Figure 6 for a case at σ=12° and an elevator deflection of 5°. The forces and moments for the complete polar are plotted in Figures 7 to 9. The predicted normal force coefficient is in excellent agreement with experiment over the entire incidence range. The computed pitching moments also agree reasonably well with experiment. However, in common with the body-wing configuration the axial force is underpredicted by approximately 25%. It is suggested that these disappointing axial force results could be due to the inadequacies of the simple algebraic turbulence model. Computations using a time-marching solver and the Spalart-Allmaras [18] one-equation turbulence model have proved to be more successful.

4 Conclusions

A PNS solver has been developed for predicting the aerodynamic characteristics of missile and projectile configurations at supersonic speeds. A multiblock approach is used to provide geometric flexibility and the ability to model realistic configurations. The code uses an iterative approach on each marching plane, which improves robustness and circumvents the need for small spatial steps. The use of implicit pseudo time iteration provides rapid convergence and enables viscous solutions to be obtained on realistic geometries in a few hours without the need for large and expensive computing resources.

The predictive performance of the solver has been evaluated using three challenging test cases. In general the results obtained are very good and most of the flow features of interest are well predicted. However, the predicted axial force is consistently found to be lower than observed in the wind tunnel. This problem is thought to be due to the simple algebraic turbulence model currently employed. A more sophisticated turbulence model would probably improve the prediction of skin friction and therefore axial force.

Acknowledgements

The work reported here was funded under the Corporate Research Programme of the UK Ministry of Defence. The authors would like to thank SAAB Dynamics for enabling them to use GEMINI during the course of this work.

References

[1] Qin N and Richards BE, Finite volume 3DNS and PNS solutions of hypersonic viscous flows around a delta wing using Osher's flux difference splitting, Proceedings of a Workshop on Hypersonic Flows for Re-entry Problems, 2, 947-959, 1990.

[2] Birch TJ, Qin N and Jin X, Computation of supersonic viscous flows around a slender body at incidence, AIAA Paper 94–1938, 1994.

[3] Shaw S and Qin N, A matrix-free preconditioned Krylov subspace method for the PNS equations, AIAA Paper 98-0111, 1998.

[4] Qin N, Ludlow DK, Zhong B, Shaw S and Birch TJ, Multigrid Acceleration of a Preconditioned GMRES Implicit PNS Solver, AIAA Paper 99-0779, 1999.

[5] Baldwin B and Lomax H, Thin-layer approximation and algebraic model for separated turbulent flows, AIAA 16th Aerospace Sciences Meeting, Huntsville, AL, Jan. 16–18, 1978.

[6] Degani D and Schiff LB, Computation of Turbulent Supersonic Flows around Pointed Bodies Having Crossflow Separation, Journal of Computational Physics, Vol. 66, pp 173–196, 1986.

[7] Qin N and Jayatunga C, Algebraic Turbulence Modelling for Vortical Flows around Slender Bodies, NATO/RTO Symposium of the Applied Vehicle Technology Panel on Missile Aerodynamics, Sorrento, Italy, May 11-15, Paper 20, 1998.

[8] Vigneron YC, Rakich JV and Tannehill JC, Calculation of supersonic viscous flows over delta wings with sharp leading edges, AIAA Paper 78–1137, 1978.

[9] Morrison JH, and Korte JJ, Implementation of Vigneron's streamwise pressure gradient approximation in the PNS equations, AIAA Paper 92-0189, 1992.

[10] Reyhner TA, and Flügge-Lotz I, The Interaction of a Shock Wave with a Laminar Boundary Layer, International Journal of Non-Linear Mechanics, Vol. 3, pp 173–199, 1968.

[11] Osher S and Solomon F, Upwind Difference Schemes for Hyperbolic Systems of Conservative Laws, Mathematics of Computation, Vol. 38, pp 339–374, 1992.

[12] Anderson WK, Thomas JL and Van Leer B, Comparison of Finite Volume Flux Vector Splittings for the Euler Equations, AIAA Journal, Vol. 24, pp 1453–1460, 1986.

[13] Saad Y and Schultz MH, GMRES: A Generalised Minimal Residual Algorithm for Solving Non-Symmetric Linear Systems, SIAM Journal on Scientific and Statistical Computing, Vol. 7, pp 856–869, 1986.

[14] Gear CW and Saad Y, Iterative Solution of Linear Equations in ODE Codes, SIAM Journal on Scientific and Statistical Computing, Vol. 4, pp 583–601, 1983.

[15] Brandt A, Multi-Level Adaptive Solutions to Boundary-Value Problems, Mathematics of Computation, Vol. 31, pp 333–390, 1977.

[16] D'Espiney P, Champigny P, Baudin D and Pilon J, Couche limite autour d'un fuselage de missile en incidence en ecoulement supersonique etude experimentale et calculs Navier-Stokes, NATO/RTO Symposium of the Applied Vehicle Technology Panel on Missile Aerodynamics, Sorrento, Italy, May 11-15, Paper 19, 1998.

[17] Sowa J, GEMINI – General missile Navier-Stokes integrator, ICAS-92-4.3.1, 1992.

[18] Spalart P and Allmaras S, A one-equation turbulence model for aerodynamic flows, AIAA Paper 92-0439, 1992.

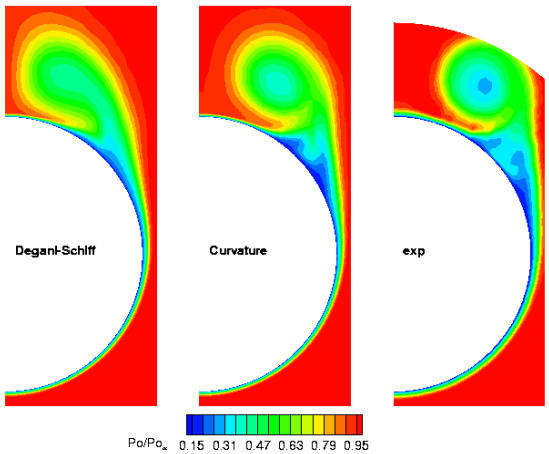

Figure 1. Measured and predicted flowfield for isolated body at M=2, s=10°, x/D=9.

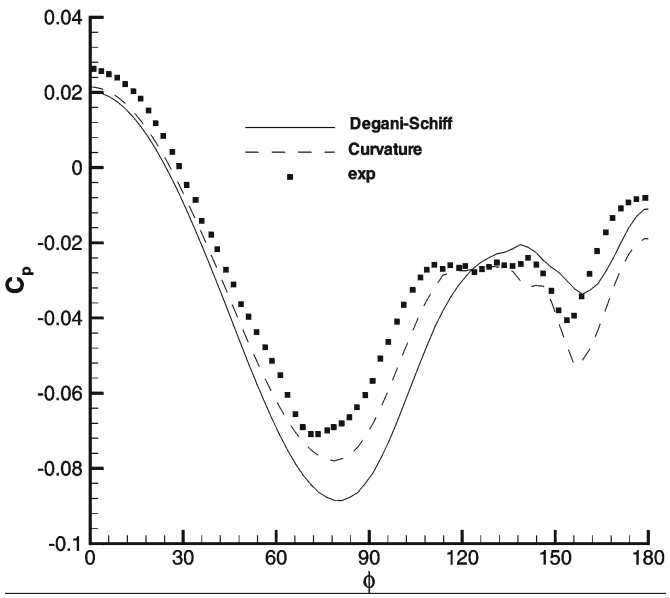

Figure 2. Measured and predicted circumferential pressure distribution for isolated body, M=2, s=10°, x/D=9.

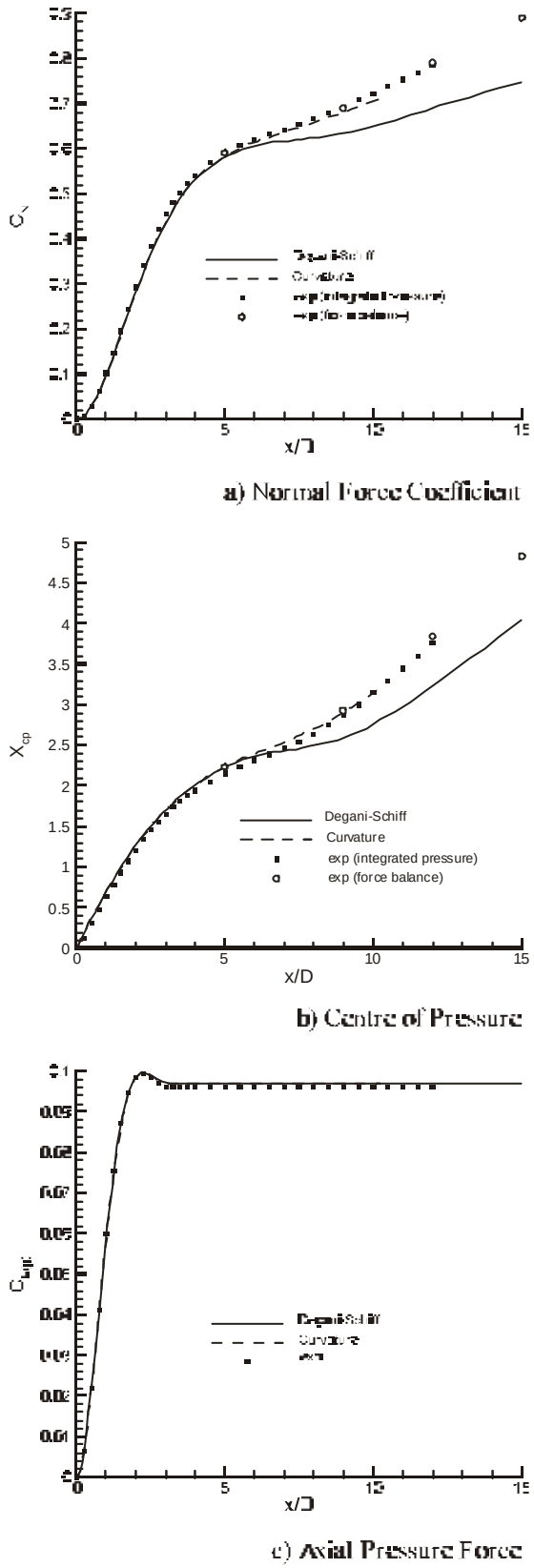

Figure 3. Measured and predicted forces and moments for isolated body at M=2, s=10°.

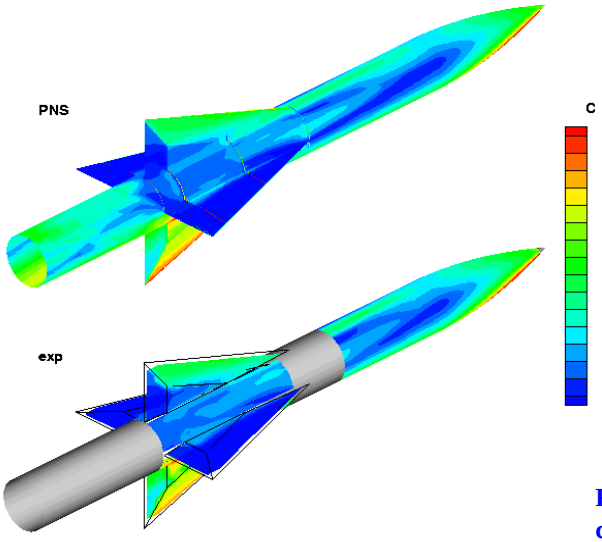

Figure 4. Measured and predicted surface pressures, M=2.5, s=14°.

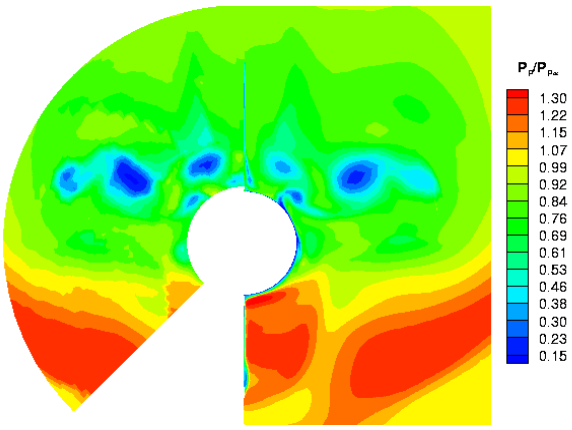

Figure 5. Measured and predicted flowfield at x/D=11.5.

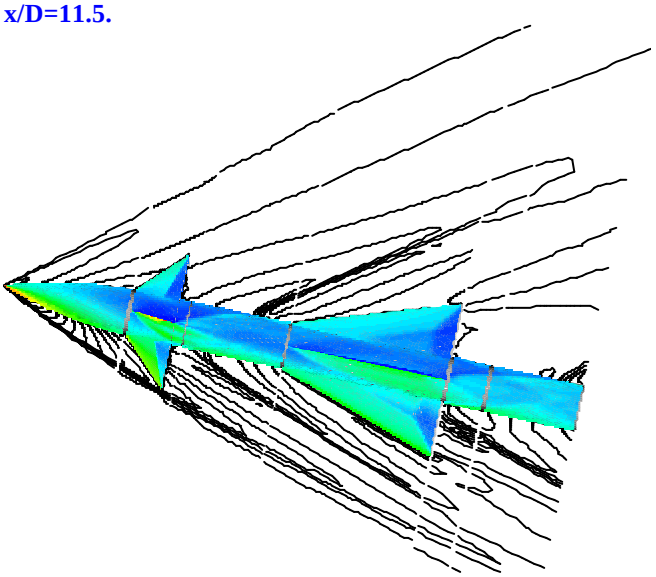

Figure 6. Predicted pressure distribution and density contours, M=2.5, s=12°, h=5°.

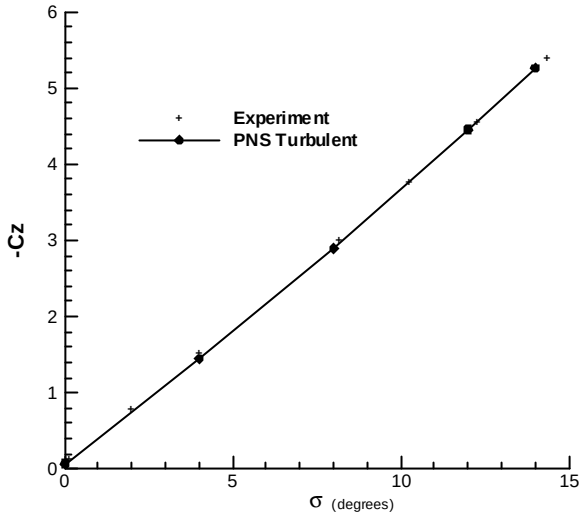

Figure 7. Normal force against incidence for body-canard-wing , M=2.5, h=5°.

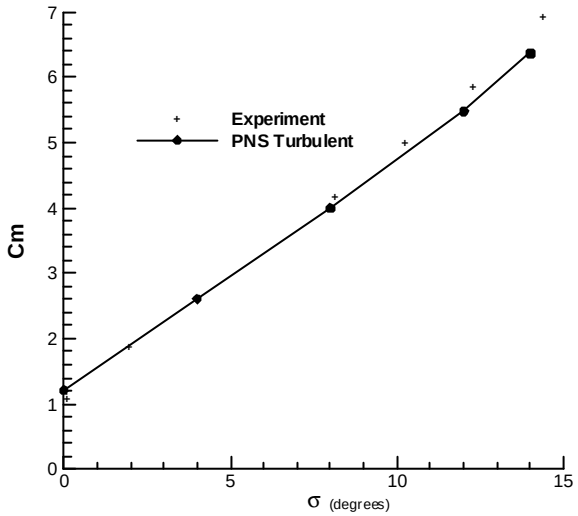

Figure 8. Pitching moment against incidence for body-canard-wing, M=2.5, h=5°.

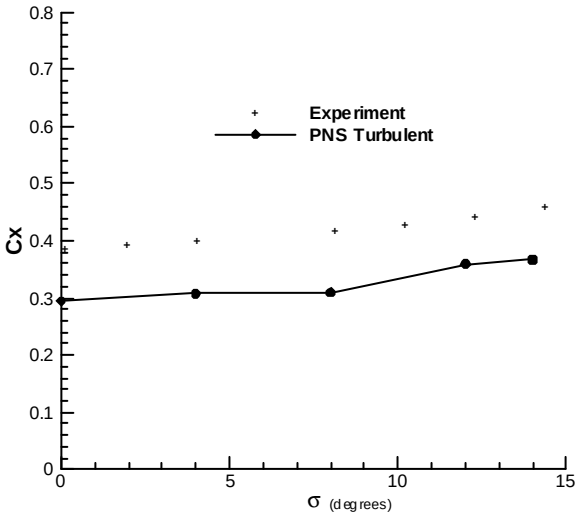

Figure 9. Axial force against incidence for body-canard-wing, M=2.5, h=5°.